THE ROYAL SOCIETY

Transmission double-crystal synchrotron studies of synthetic diamond using the Haruta stereo-pairs technique

By Moreton Moore and W. Wierzchowski†

Department of Physics, Royal Holloway, University of London, Egham Hill, Egham, Surrey TW20 0EX, UK

The Haruta method of obtaining a stereoscopic effect by a small rotation about the diffraction vector was used for the first time in the case of synchrotron X-ray double-crystal topography.

Double-crystal experiments were performed on a $1.5 \times 4 \times 4\,\mathrm{mm}^3$ slab cut from a cuboctahedral synthetic diamond in the arrangement where the asymmetric 220 diamond reflection was matched by the 331 reflection from a silicon monochromator selecting 1.0 Å radiation. The double-crystal topographs provided intense contrast for dislocations, stacking faults, growth-sector boundaries and other defects, often accompanied by distinct interference fringes. The images were strongly angle dependent and appropriate Haruta pairs were matched from series taken at positions on the rocking curve separated by small increments.

The pairs exhibited a good stereoscopic effect for most of the defects, and also for the cases of many interference fringes. The stereoscopic effects were also compared with those obtained in single-crystal Haruta pairs in exactly the same geometry. It was found that some fringes, associated with some growth-sector boundaries and stacking faults, did not, however, produce a good stereoscopic effect, but the fringes appeared visible on the exit surface. These various features were confirmed by simulation of the stereoscopic effects in computer-calculated images of dislocations and stacking faults.

Keywords: diamond; crystal defects; dislocations; stereo pairs; synchrotron radiation; X-ray topography

1. Introduction

Stereoscopic techniques offer great assistance in establishing the geometry of defects, especially when in large concentrations and in complicated configurations. An exceptionally convenient way of obtaining a pair of X-ray topographs, suitable for producing a stereoscopic effect, was proposed by Haruta (1965). This method consists of making a pair of topographs differing by a small rotation about the diffraction vector, symmetrically disposed around the central position. The two topographs correspond to the observation of the defects by different eyes, and when viewed using a stereoscope they produce the desired effect. The advantage of the Haruta method

† Permanent address: Institute of Electronic Materials Technology, Wólczyńska 133, 01-919 Warsaw, Poland.

is in producing topographs with equivalent contrast, which may not be the case if using different diffraction vectors. The suitable angle of rotation is dependent on the actual thickness of the crystal (Lang 1978). The Haruta-pair technique is normally used in the case of single-crystal projection topography but its application in section topography has also been described by Lang (1978).

In the present paper we used the Haruta-pair technique for transmission synchrotron double-crystal topography of diamond. It is well known that transmission double-crystal topographs provide images of similar character to transmission single-crystal projection topographs. Both methods produce images with dominating dark direct contrast in cases of low absorption and dominating dynamical contrast at higher absorption. The differences consist of much greater extension of the defect image and in the critical dependence of the image on the rocking-curve angle. A common feature of transmission double-crystal images is also the much greater number of interference fringes, whose visibility and dependence on the rocking-curve angle become more distinct with reduction of the divergence of the incident beam formed by the monochromator.

The idea of the use of the Haruta-pair technique in transmission double-crystal topography was associated with obtaining in an earlier experiment some very impressive images, exhibiting many details and numerous interference fringes. These interference fringes appeared in the images of dislocations, stacking faults and also on some growth-sector boundaries. The formation mechanism of some of these diffraction fringes was not clear and information concerning the location of crystal details connected with these fringes inside the crystal was important.

The results of the double-crystal investigation were compared with the single-crystal Haruta pairs and section topographs intersecting the crystal in various places. We also refer to our other investigation performed on the present diamond (Wierzchowski *et al*. 1991). Some preliminary results of our present experiments were published as a conference paper (Moore *et al*. 1994).

2. Experimental

The investigated sample was a $1.5 \times 4 \times 4\,\mathrm{mm}^3$ slab prepared from a synthetic diamond grown by the Sumitomo Electric Company by polishing off the upper and lower parts. The specimen was thus bounded by two artificially introduced surfaces perpendicular to the main [001] grown direction. It was grown by the reconstitution method (Strong & Wentorf 1972), essential for obtaining large-diameter diamonds of good crystallographic perfection. Similar diamonds grown by Sumitomo have been described by Shigley *et al*. (1986). The sample was kindly loaned to us by Professor A. T. Collins.

The double-crystal Haruta pairs of topographs were obtained at Station 7.6 of the Synchrotron Radiation Source at CLRC Daresbury Laboratory (UK). The double-crystal experiments were performed using an arrangement with the asymmetric 220 reflection from the investigated diamond matched by the 331 reflection from a (110)-oriented silicon monochromator. This arrangement selected 1.0 Å radiation.

The investigated sample had been subjected formerly to a number of different examinations (Wierzchowski *et al*. 1991), including systematic studies of diffraction configuration from Lang projection topographs taken in 111-type and 220-type reflections from all four equivalent {111} and all six equivalent {110} crystallographic

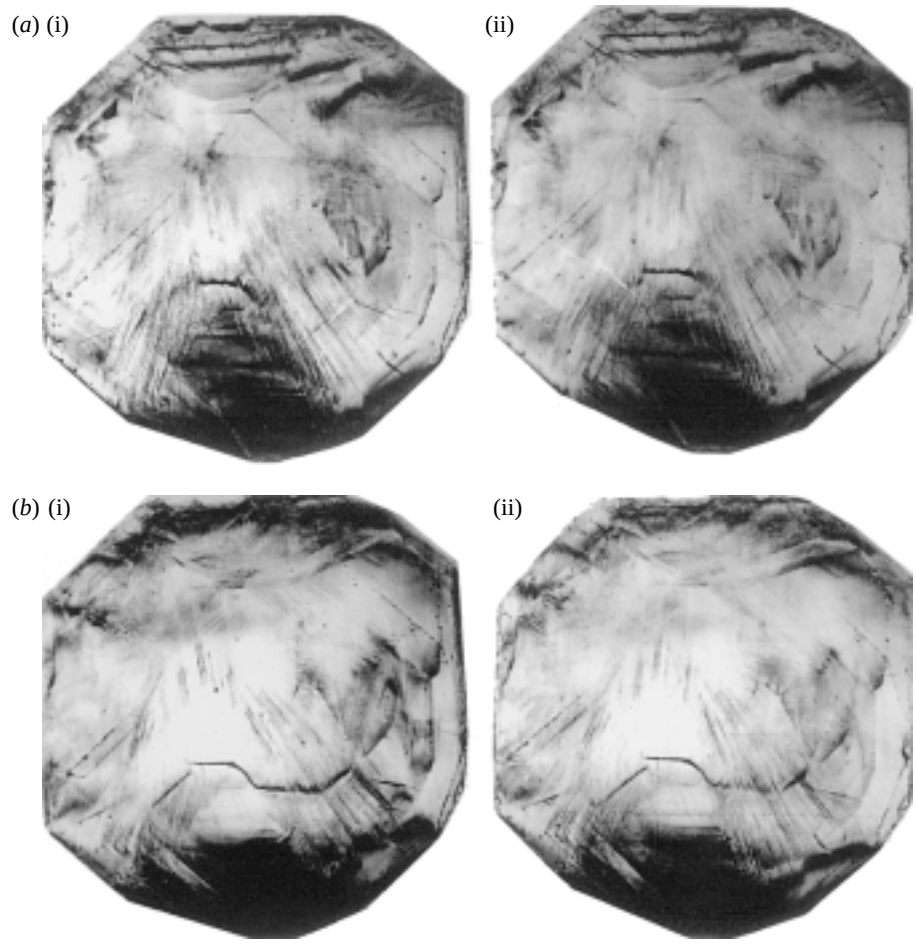

Figure 1. Two (a, b) representative Haruta stereoscopic pairs of synchrotron double-crystal transmission topographs of a Sumitomo synthetic diamond, taken in the asymmetric 220 reflection of 1.0 Å radiation. The angular displacement between (a) and (b) is 1.5 arc seconds. A stereoscopic effect may be achieved by using a stereo-viewer with lenses of focal length 7–10 cm for each pair ((i) and (ii)).

planes in Mo Kα_1 radiation. We also performed some other double-crystal investigations, both with synchrotron and conventional source arrangements. These investigations allowed us to determine the orientation and crystallographic type of dislocations and stacking faults present in the diamond. They also provided some evaluation of the lattice parameter differences between growth sectors in the present diamond.

The greatest difficulty in obtaining a good stereoscopic effect was associated with the critical dependence of the topographs on the angular setting. It was necessary to expose and to match pairs of topographs at equivalent positions on the rocking curve, and differing only by slightly different projections of the image. One practicable method was to match appropriate pairs from the numerous topographs of a series, obtained at angular intervals of small step size, passing through the peak setting.

The present Haruta-pair experiment was realized with a tilting angle of rotation

about the diffraction vector equal to $\pm 2.5°$. The numerous series of topographs were exposed with the angular setting altered by 0.5 arc seconds, with more than 18 topographs in each series passing through the peak. Such extensive series enabled us to achieve better stability of the experimental arrangement. Making use of such dense series, we were able to find matched pairs corresponding to equivalent places on the rocking curve and hence providing a good stereoscopic effect.

As a comparative reference point we also took synchrotron single-crystal Haruta pairs of topographs, using the equivalent orientation and reflection with the same Bragg angle, selecting 1.0 Å radiation. As may be evaluated from the spectral distribution of synchrotron radiation, the contribution of harmonics to these single-crystal topographs is not entirely negligible, but it is probably only a third of those produced by 1.0 Å radiation.

Some further investigations were performed in order to explain the possible mechanism of generation of some interference fringes. Apart from the experiments with section and double-crystal topography described earlier, we exposed series of synchrotron section topographs in the geometry corresponding to the present Haruta-pair experiments (i.e. with the same asymmetric 220 reflection of 1.0 Å radiation).

The crystal was also studied with 440 and 220 Mo Kα_1 projection topographs and by limited projection topographs from the same set of reflecting planes. The limited projection topographs revealed the defect structures of regions lying close to the entrance and exit surfaces of the crystal in the 440 and 220 reflections, respectively. We also obtained similar fringes in double-crystal topographs taken in the $331_{\mathrm{Si}}, -220_{\diamond}$ arrangement with Mo Kα_1 radiation.

Some further information concerning the defects in the region producing the fringes was obtained from the high-resolution back-reflection synchrotron double-crystal topographs taken with the 004 reflection from the large artificial surface further from the seed. In this arrangement the diamond 004 reflection was matched by the $53\overline{1}$ reflection from a (111)-oriented silicon monochromator and the arrangement selected 1.35 Å radiation. Some of these topographs taken on the tails of the rocking curve were characterized by considerable penetration depth and the revealing of fringe patterns in the images of some defects. These topographs were very helpful in revealing that some stacking faults were taking part in the formation of the fringes.

3. Experimental results

Just two representative Haruta pairs of the many double-crystal topographs of the Sumitomo diamond, which may be used for stereoscopic observation, are shown in figure 1. These topographs can be combined for stereoscopic viewing using a single lens with 3–4 cm focal length in front of each eye. An equivalent Haruta pair of single-crystal projection topographs is shown in figure 2. For better understanding of the topographs, a diagram showing the corresponding projection of the diamond and the position of the diffraction vector is given in figure 3. The diffracted beam exits mainly through the artificial (001) face further from the seed, and the topographs revealed dominantly the defects closer to this side of the crystal.

The defect structure of the sample has been discussed in detail in our other paper (Wierzchowski *et al.* 1991). The crystal was of cuboctahedral habit with considerable {113} growth faces. The two artificial surfaces intersected a complicated pattern of growth sectors, which were best revealed with back-reflection double-crystal topog-

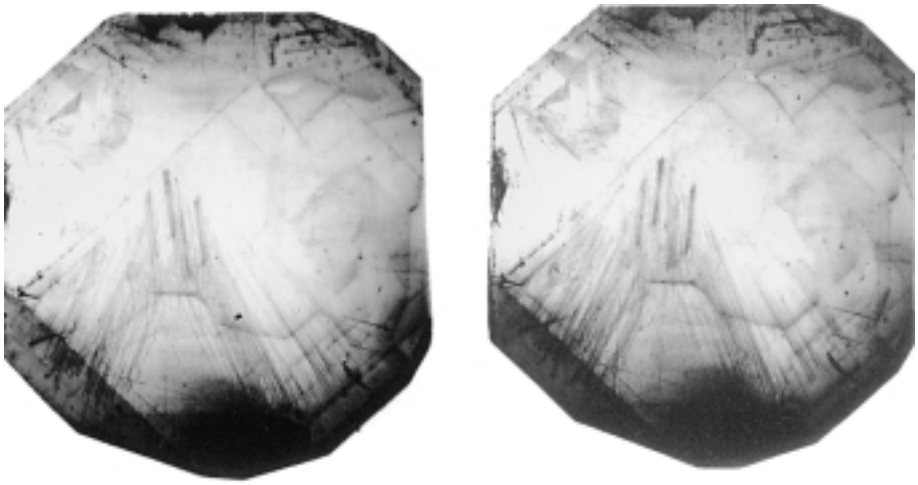

Figure 2. A Haruta pair of synchrotron single-crystal topographs of the Sumitomo diamond taken in the same 220 reflection of 1.09 Å radiation.

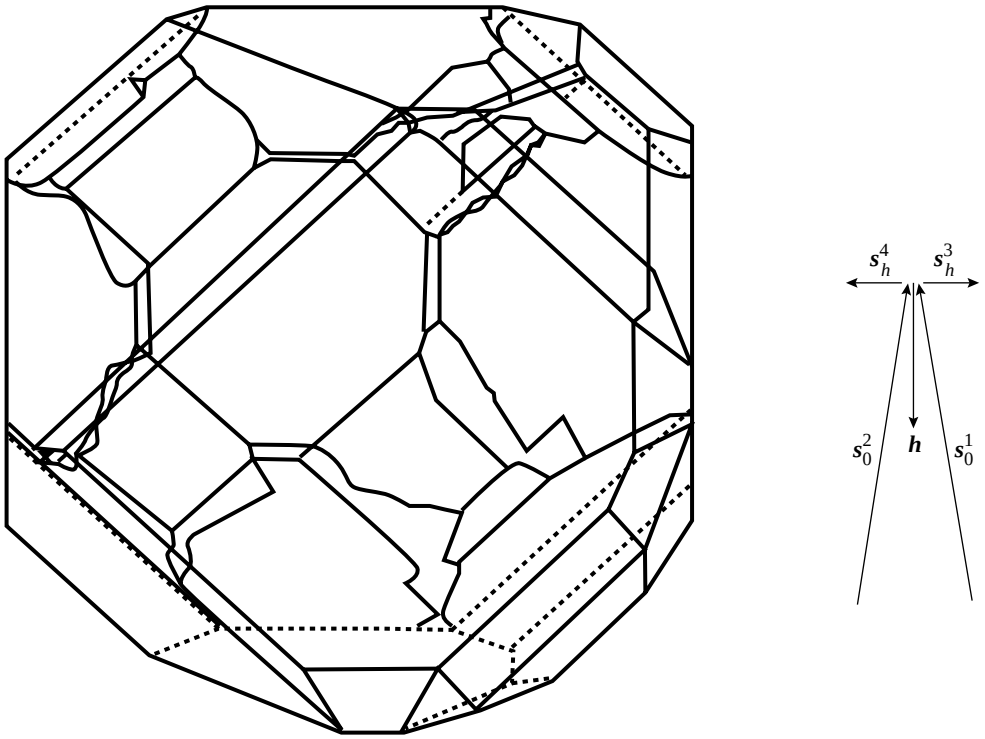

Figure 3. A perspective drawing of the Sumitomo diamond corresponding to that of the topographs in figures 1 and 2, with the directions of the incident and reflected beams shown. For identification of details, the growth-sector boundaries on the polished surfaces are marked by thin lines.

raphy and by cathodoluminescence microscopy. In the topographs shown here we can see approximately half of the dislocations present in the crystal, grouped preferentially into bundles. It was found from the point of intersection of the extrapolated dislocation bundles that the present surface of the crystal had been cut *ca.* 1 mm from the original seed crystal. The second artificial surface cut off some small {011} facets, but it was introduced not very far from the upper growth (001) face, as the central (001) sector dominates on this face.

The observed dislocations and bundles were related to some growth sectors according to the rule that the predominant orientation of each dislocation line is perpendicular to the growing face. The dominant orientation of bundles is ⟨112⟩, related to {113} and {111} sectors. However, we observed bundles and individual dislocations also lying in the ⟨011⟩ and ⟨001⟩ directions. In particular, some bundles lying along [001] directions are present in the central (001) sector. Short segments of grown-in dislocations are revealed in the single- and double-crystal Haruta pairs of topographs.

The most common types of dislocations identified from the projection topographs were mixed-type 30° and edge dislocations along the ⟨112⟩ directions, and mixed-type 60° dislocations along the ⟨011⟩ directions. We also found in the present crystal some kinked dislocations. It also contains a number of stacking faults, especially populated close to octahedral faces.

It may be noticed that the images of defects in the double-crystal topographs are much more intense than in the single-crystal topographs, and that they contain more interference fringes. In particular the fringes form dots along the dislocation lines that are invisible in the single-crystal topographs. The fringes on the stacking faults are visible by both methods, but those in the double-crystal topographs are more distinct, and are dependent upon the angular setting.

The diamond contains a complex pattern of growth sectors, with a number of sectors surrounding the major central (001) sector. The single-crystal topographs revealed only part of the growth-sector boundary outcrops on the artificially polished surfaces. These boundaries are marked with thin lines in figure 3. In addition, the double-crystal topographs revealed interference fringes corresponding to the boundaries of the central growth sector inside the crystal. The above-mentioned defects produced a good stereoscopic effect. This applies also to the fringes along dislocations and to the fringes on the stacking faults, and to the boundaries of the central sector.

Our particular attention was devoted to a system of fringes that appeared in the upper right part of the image shown in figure 1*a*. In stereoscopic observation, this system appeared to be localized on the exit surface. The analysis of all the topographic investigations performed indicates that this system of fringes is caused by the boundary between {100} and {011} growth sectors and a stacking fault. These objects are situated near to the other surface, closer to the seed. They may be associated with the aforementioned fringes and they were observed in other sections and double-crystal topographs (not shown here).

The appearance of the fringes on the exit surface is explainable by noting that a good stereoscopic effect is obtained when the details of the image are produced by radiation propagating inside the crystal close to the direction of the reflected beam. A good stereoscopic effect can take place especially for fringes formed due to the interference of wave-fields with excitation points situated close to the centre of the dispersion hyperbola.

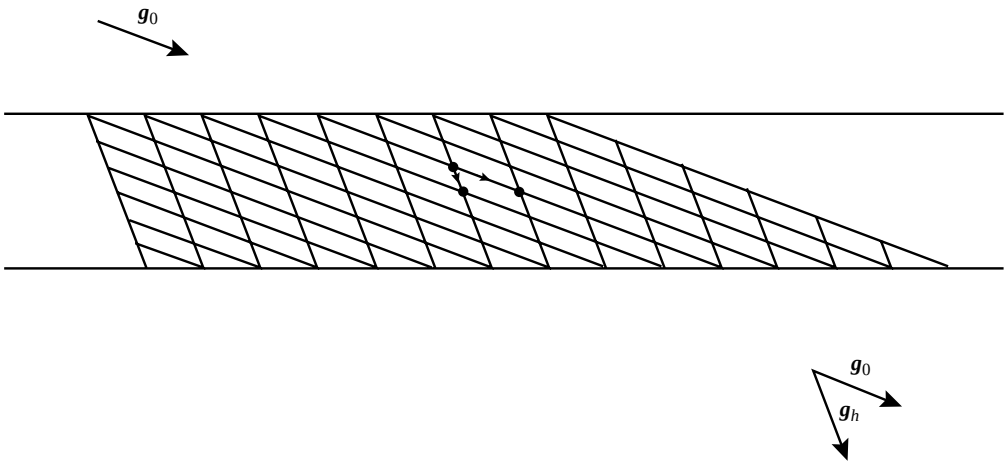

Figure 4. The grid of numerical integration suitable for obtaining the simulations of transmission plane-wave topographs from a parallel-sided slab.

4. Investigation of stereoscopic effect in numerical simulation

It was expected that some assistance in discussing the observed stereoscopic effect associated with different types of interference fringes could be provided by the use of a numerical simulation of the images. For the analysis of the stereoscopic effects, we performed simulations of the dislocation images and the stacking faults that seemed to correspond to the two most important cases of diffraction fringes observed here.

A necessary simplification used in the present simulations was the approximation of the crystal by a parallel-sided slab. The present experiment in principle corresponded to plane-wave topography and the simulation was based upon the numerical integration of the Takagi–Taupin equations, first performed by Taupin (1967) and Authier *et al*. (1968). The corresponding integration grid, shown in figure 4, and the half-step derivative method were used. Thanks to the much improved performance of modern computers, it was possible also to take into account the divergence of the monochromatized beam by adding at least 40–80 wave simulations with small increments in the angle of incidence, weighted by the intensity of the typical reflection curve (Wierzchowski *et al*. 1995). It was also possible to perform simulations corresponding to single-crystal topographs, adding without weighting at least 200 plane-wave topographs covering an angular range four times greater than the full-width-at-half-maximum (FWHM) of the actual reflection.

The required stereoscopic effect was obtained by appropriate turning of the dislocation or the stacking fault in the sense opposite to the turning of the crystal between exposures of the experimental Haruta pairs. As in the case of our other paper (Wierzchowski *et al*. 1995), we calculated the effective change of the Bragg angle according to Shaibani & Hazzledine (1981). The simulation of the stacking fault image was realized by introducing changes in the Fourier coefficient of the dielectric susceptibility in the second part of the crystal, shifted with respect to the first, by the stacking fault vector $\boldsymbol{f}$ (Authier 1968):

$$\chi'_h = \chi_h \exp(2\pi \mathrm{i} \boldsymbol{h} \cdot \boldsymbol{f}), \quad \chi'_{\bar{h}} = \chi_{\bar{h}} \exp(-2\pi \mathrm{i} \boldsymbol{h} \cdot \boldsymbol{f}). \tag{4.1}$$

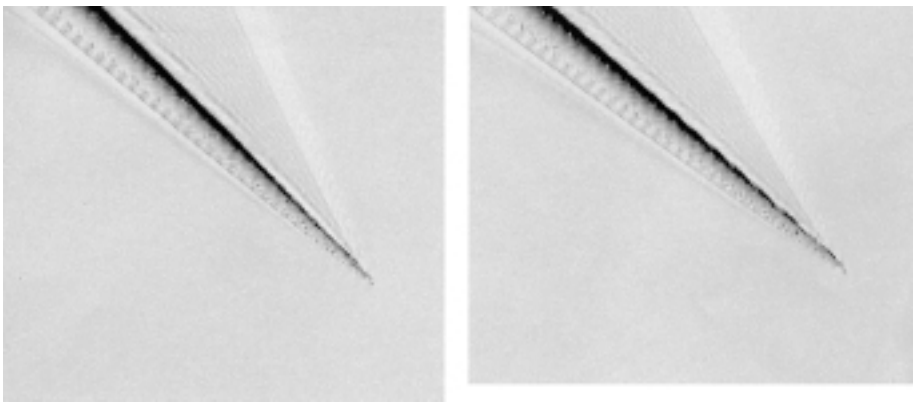

Figure 5. Haruta pairs of simulated images of dislocations, showing a good stereoscopic effect, corresponding to the present double-crystal experiment, by taking into account the finite divergence of the beam.

A representative simulation of a stereoscopic Haruta pair of dislocations is shown in figure 5. Simulations corresponding to plane-wave topographs were computed (but are not shown here) and also to topographs taking into account the real divergence of the monochromatized beam. The good stereoscopic effect of dislocation images and their associated interference fringes may be seen by observation of the simulations or by checking that the most distinct parts of dislocation images are in fact analogous to direct contrast, i.e. that they come from the neighbourhood of the dislocation core and are reproduced along the direction of the reflected beam.

A stereoscopic effect was not so evident in the case of simulated images of the stacking fault, where the stacking fault was oblique to the plane of diffraction and the images appeared on the surface of the crystal.

5. Conclusions

The Haruta-pair technique has been applied to the stereoscopic observation of diamond in double-crystal topographs, we believe for the first time. Suitable pairs, corresponding to equivalent points on the rocking curve, were matched from series of topographs taken with angular settings separated by small increments.

The attainment of good stereoscopic images from most of the defects is of considerable practical importance in view of their high sensitivity and the revelation of more details than in the case of single-crystal topography. An example was found of the appearance of interference fringes distant from their origin, indicating the propagation of wave-fields far from the reflected beam direction.

It was also possible to create the Haruta-pair topographs by numerically simulated images of dislocations and stacking faults. The obtained Haruta pairs confirmed a good stereoscopic effect in the case of dislocations but a relatively poor stereoscopic effect in the case of the stacking fault images.

The authors thank the director and staff of the CLRC Daresbury Laboratory (UK) for the provision of synchrotron experimental facilities, the Engineering and Physical Sciences Research Council (EPSRC) for a research grant, Professor A. T. Collins (King's College London) for the loan of the specimen and Mr A. P. W. Makepeace for assistance in some of the experiments.

References

Authier, A. 1968 *Physica Status Solidi* **27**, 77–93.

Authier, A., Malgrange, C. & Tournarie, M. 1968 *Acta Crystallogr.* A **24**, 126.

Haruta, K. 1965 *J. Appl. Phys.* **36**, 1789–1790.

Lang, A. R. 1978 In *Diffraction and imaging techniques in material science* (ed. S. Amelinckx, R. Gevers & J. van Landuyt), pp. 623–714. Amsterdam: North-Holland.

Moore, M., Lang, A. R. & Wierzchowski, W. 1994 *Acta Phys. Pol.* A **86**, 613–616.

Shaibani, S. J. & Hazzledine, P. M. 1981 *Phil. Mag.* A **44**, 657–665.

Shigley, J. E., Fritsch, E., Stockton, C. M., Koivula, J. I., Fryer, C. W. & Kane, R. E. 1986 *Gems Gemmology* **22**, 192.

Strong, H. M. & Wentorf Jr, R. H. 1972 *Naturwissenschaften* **59**, 1–7.

Taupin, D. 1967 *Acta Crystallogr.* **23**, 25.

Wierzchowski, W., Moore, M., Makepeace, A. & Yacoot, A. 1991 *J. Cryst. Growth* **114**, 209–227.

Wierzchowski, W., Mazur, K. & Wieteska, K. 1995 *J. Phys.* D **28**, A33–A37.